



UCRL-ID-114037

PCMDI Report No. 20

**THE NORTHERN WINTERTIME DIVERGENCE
EXTREMA AT 200 hPa AND SURFACE CYCLONES
AS SIMULATED IN THE AMIP INTEGRATION
OF THE ECMWF GENERAL CIRCULATION MODEL**

by

James S. Boyle

Program for Climate Model Diagnosis and Intercomparison
Lawrence Livermore National Laboratory, Livermore, CA, USA

November 1994

**PROGRAM FOR CLIMATE MODEL DIAGNOSIS AND INTERCOMPARISON
UNIVERSITY OF CALIFORNIA, LAWRENCE LIVERMORE NATIONAL LABORATORY
LIVERMORE, CA 94550**

DISCLAIMER

This document was prepared as an account of work sponsored by an agency of the United States Government. Neither the United States Government nor the University of California nor any of their employees, makes any warranty, express or implied, or assumes any legal liability or responsibility for the accuracy, completeness, or usefulness of any information, apparatus, product, or process disclosed, or represents that its use would not infringe privately owned rights. Reference herein to any specific commercial products, process, or service by trade name, trademark, manufacturer, or otherwise, does not necessarily constitute or imply its endorsement, recommendation, or favoring by the United States Government or the University of California. The views and opinions of authors expressed herein do not necessarily state or reflect those of the United States Government or the University of California, and shall not be used for advertising or product endorsement purposes.

This is an informal report intended primarily for internal or limited external distribution. The opinions and conclusions stated are those of the author and may or may not be those of the Laboratory.

This report has been reproduced
directly from the best available copy.

Available to DOE and DOE contractors from the
Office of Scientific and Technical Information
P.O. Box 62, Oak Ridge, TN 37831
Prices available from (615) 576-8401, FTS 626-8401

Available to the public from the
National Technical Information Service
U.S. Department of Commerce
5285 Port Royal Rd.,
Springfield, VA 22161

ABSTRACT

Divergence and convergence centers at 200 hPa and mean sea level pressure (MSLP) cyclones were located every 6 hr for a 10-yr general circulation model (GCM) simulation with the ECMWF (Cycle 36) for the boreal winters from 1980 to 1988. The simulation used the observed monthly mean sea surface temperature (SST) for the decade. Analysis of the frequency, location, and strength of these centers and cyclones gives insight into the dynamical response of the model to the varying SST.

The results indicate that (1) the model produces reasonable climatologies of upper-level divergence and MSLP cyclones; (2) the model distribution of anomalies of divergence and convergence centers and MSLP cyclones is consistent with observations for the 1982–83 and 1986–87 El Niño events; (3) the tropical Indian Ocean is the region of greatest divergence activity and interannual variability in the model; (4) the variability of the divergence centers is greater than that of the convergence centers; (5) strong divergence centers occur chiefly over the ocean in the midlatitudes but are more land-based in the tropics, except in the Indian Ocean; and (6) locations of divergence and convergence centers can be a useful tool for the intercomparison of global atmospheric simulations.

1. Introduction

The Atmospheric Model Intercomparison Project (AMIP) of the World Climate Research Programme's Working Group on Numerical Experimentation (WGNE) is an ambitious attempt to comprehensively intercompare atmospheric general circulation models (GCMs) in use by forecasting and research groups all over the world (Gates, 1992). The modeling groups participating in AMIP (of which there are about 30) each simulate the global atmosphere for the decade 1979 to 1988, using a common solar constant, CO₂ concentration, monthly averaged sea surface temperature (SST), and sea ice data set. This project provides an unprecedented opportunity for realistic and detailed validation and intercomparison of current GCMs. This paper presents the results of our studies of large-scale centers of divergence and convergence at 200 hPa and mean sea-level pressure (MSLP) cyclones during the northern winter for one of these GCM simulations. This work represents a pilot study of an intercomparison that could be undertaken for the full suite of AMIP GCM simulations.

This work was inspired in part by the paper of Hsu and Lin (1993), who analyzed global teleconnection patterns using the 250-hPa streamfunction. Earlier works used the 500-hPa geopotential to establish the teleconnection patterns and were restricted to the Northern Hemisphere extratropics. By using the streamfunction, Hsu and Lin were able to establish global patterns across the tropical latitudes, where geostrophy does not dominate the dynamics. The idea in the present work is to perform a global analysis of what can be termed storminess or unsettled weather. At the higher latitudes, where geostrophy dominates, MSLP minima are often used to identify storms. In the tropics, the upper-level divergence and the associated velocity potential are often used to diagnose unsettled conditions and systems of interest. The upper-level divergence (convergence) was regarded as a variable of global significance that effectively summarizes much of a model's dynamics and its response to varying SST. The upper-level divergence is intimately linked to the vertical motion field and is a common factor in precipitation-producing systems in both midlatitudes and the tropics. Since the ultimate use of this analysis will be in the comparison of simulations by different models, the sensitivity of the upper-level divergence to the model parameterizations is an advantage; effective model comparison requires a variable that will draw clear distinctions among the behaviors of the models.

A drawback to using the divergence is the dearth of verification data. There are no commonly agreed-to, reliable analyses of the day-to-day variation in the irrotational

wind. However, the reanalysis projects at the European Centre for Medium-Range Weather Forecasts (ECMWF) and the National Meteorological Center (NMC) (Kalnay and Jenne, 1991) may provide a dynamically consistent best estimate of the divergent wind. In the present work, qualitative comparisons are made using proxy verification data, such as cyclone frequency in midlatitudes and in the tropics, highly reflective cloud variations, and outgoing longwave radiation.

There is a long history of identifying cyclone and anticyclone centers on sequences of MSLP charts and plotting the resulting frequencies and contours (Petterssen, 1956; Whittaker and Horn, 1983). These plots often give insight into the mechanism of cyclone generation and maintenance and into the individual system's relation to the time mean general circulation patterns of wind and temperature. Comparison of GCM output with the observed cyclone distribution is a useful evaluation tool for the models in that it provides a check that the synoptic systems in the model are behaving in a fashion similar to that of the atmosphere. Lambert (1988) performed such a comparison for the Canadian Climate Model. The use of sea-level pressure to identify storm systems essentially restricts the usefulness of such studies to midlatitudes, since tropical systems typically have relatively small pressure perturbations. In addition, the use of MSLP is questionable in regions of elevated terrain because of inconsistencies in procedures for reduction to sea-level pressure. In this paper, MSLP cyclone frequencies have been calculated, and these data form a basis for comparing the divergence centers with the more established diagnostic. There is some ambiguity in relating MSLP cyclones and upper-level (200-hPa) divergence, since for any given storm the signal at 200 hPa could be weak or nonexistent. In addition, the upper-level divergence might be prominent for only a limited portion of the life of a cyclone. Nevertheless, on the average, the upper-level divergence will be an identifying feature associated with the surface cyclone activity. The relation is not one-to-one but is undoubtedly significant.

In the tropics, where MSLP is a poor indicator of storms, precipitating features have often been identified in satellite imagery as regions of highly reflective cloud (HRC) or minima in the outgoing longwave radiation (OLR). These proxy measures are essentially trying to estimate where the divergence is located on the basis of the location of vertically developed thick clouds. Again, this comparison is useful but not perfect.

2. Model and Experiment Description

The model used for this experiment was the ECMWF operational model, Cycle 36. This model has 19 levels in the vertical and, for this experiment, was set to a horizontal resolution of T42. The model is in all respects the same as that described by Miller et al. (1992). This version of the model uses a gravity wave drag parameterization and a convective mass flux scheme. The T42 resolution is a compromise between the conflicting demands of sufficient resolution and realistic computation time. The work of Tibaldi et al. (1991) indicates that the T42 resolution is adequate for the type of study performed here. In the 1979 to 1988 AMIP simulation used here, the SST and sea-ice distribution used were the observed monthly values prepared for AMIP by the Center for Ocean, Land and Atmosphere at the University of Maryland and the NOAA Climate Analysis Center. The surface land temperature and moisture are allowed to vary freely in accordance to the model's surface parameterizations. The integration began with the ECMWF analysis for 1 January 1979.

3. Analysis Technique

a. 200-hPa Divergence

The upper-level wind data from the model integration were archived every 6 hr; from these data the divergence was computed and smoothed to a resolution of T30. Use of the smoothed divergence simplifies the search for maxima and minima somewhat, although small-scale divergence centers will not be detected. For the period 15 November to 15 March, the divergence fields were searched for maxima and minima, and the position of each extremum and the corresponding divergence were recorded. The criterion for an extremum was that the central point of a 5×5 array of points had to have a divergence less (or greater) than all the surrounding points. Since the grid spacing was about 2.5° in latitude and longitude, the extremum had to be at least 10° in extent to be identified. The level chosen for this work was the 200-hPa surface. This upper level is a compromise, in that a lower level would be preferable in the midlatitudes, but an upper tropospheric level is needed to capture the outflow of deep convective systems in the tropics. This upper level was also chosen in an attempt to obviate the effects of topography on the interpolation of the model's data to pressure surfaces from the model coordinates.

It should be noted that this procedure makes no distinction between stationary or slow-moving systems and fast-moving migratory storms. A stationary system will be counted more than once during its lifetime, and will thus contribute to high frequencies where such systems are endemic. The search criterion applied at 200 hPa selects only large-scale deep systems, and this must be kept in mind when interpreting the results. These restrictions on the search may be an advantage in that they focus attention on the vigorous systems that would be expected to make a substantial impact on the general circulation statistics and climatology of the model. Another possible problem is that the 200-hPa surface goes into the stratosphere at the higher latitudes. Examination of model north-south cross sections of temperature and wind (not shown) indicates that this is not a serious problem below 60° latitude.

The analysis was carried out for the 15 November through 15 March winter seasons beginning November 1980 and ending March 1988.

b. Mean Sea-Level Pressure Minima

For the same time sequence as for the 200-hPa wind field, the MSLP was calculated using the reduction procedures used at the ECMWF. MSLP minima were located and their positions recorded using the cyclone locator code developed at the University of Melbourne and described by Murray and Simmonds (1991). This code can locate both open and closed systems, and the results described here include both types. Experiments identifying only closed systems indicated little impact on the overall results. As in the divergence centers, there is no attempt to distinguish stationary and mobile systems. Once the locations were tabulated, the data were binned in $5^\circ \times 5^\circ$ squares and normalized by area and time as for the 200-hPa divergence centers.

c. Normalizations

The locations of the centers of both the MSLP and the 200-hPa divergence were binned into $5^\circ \times 5^\circ$ squares, and the number was normalized by the area of the square at the equator. Since the area of a 5° equatorial square is about 308,000 km² and the number of centers was summed over each season, the units of the frequency are events per season and per 308,000 km².

2. Model and Experiment Description

The model used for this experiment was the ECMWF operational model, Cycle 36. This model has 19 levels in the vertical and, for this experiment, was set to a horizontal resolution of T42. The model is in all respects the same as that described by Miller et al. (1992). This version of the model uses a gravity wave drag parameterization and a convective mass flux scheme. The T42 resolution is a compromise between the conflicting demands of sufficient resolution and realistic computation time. The work of Tibaldi et al. (1991) indicates that the T42 resolution is adequate for the type of study performed here. In the 1979 to 1988 AMIP simulation used here, the SST and sea-ice distribution used were the observed monthly values prepared for AMIP by the Center for Ocean, Land and Atmosphere at the University of Maryland and the NOAA Climate Analysis Center. The surface land temperature and moisture are allowed to vary freely in accordance to the model's surface parameterizations. The integration began with the ECMWF analysis for 1 January 1979.

3. Analysis Technique

a. 200-hPa Divergence

The upper-level wind data from the model integration were archived every 6 hr; from these data the divergence was computed and smoothed to a resolution of T30. Use of the smoothed divergence simplifies the search for maxima and minima somewhat, although small-scale divergence centers will not be detected. For the period 15 November to 15 March, the divergence fields were searched for maxima and minima, and the position of each extremum and the corresponding divergence were recorded. The criterion for an extremum was that the central point of a 5×5 array of points had to have a divergence less (or greater) than all the surrounding points. Since the grid spacing was about 2.5° in latitude and longitude, the extremum had to be at least 10° in extent to be identified. The level chosen for this work was the 200-hPa surface. This upper level is a compromise, in that a lower level would be preferable in the midlatitudes, but an upper tropospheric level is needed to capture the outflow of deep convective systems in the tropics. This upper level was also chosen in an attempt to obviate the effects of topography on the interpolation of the model's data to pressure surfaces from the model coordinates.

It should be noted that this procedure makes no distinction between stationary or slow-moving systems and fast-moving migratory storms. A stationary system will be counted more than once during its lifetime, and will thus contribute to high frequencies where such systems are endemic. The search criterion applied at 200 hPa selects only large-scale deep systems, and this must be kept in mind when interpreting the results. These restrictions on the search may be an advantage in that they focus attention on the vigorous systems that would be expected to make a substantial impact on the general circulation statistics and climatology of the model. Another possible problem is that the 200-hPa surface goes into the stratosphere at the higher latitudes. Examination of model north-south cross sections of temperature and wind (not shown) indicates that this is not a serious problem below 60° latitude.

The analysis was carried out for the 15 November through 15 March winter seasons beginning November 1980 and ending March 1988.

b. Mean Sea-Level Pressure Minima

For the same time sequence as for the 200-hPa wind field, the MSLP was calculated using the reduction procedures used at the ECMWF. MSLP minima were located and their positions recorded using the cyclone locator code developed at the University of Melbourne and described by Murray and Simmonds (1991). This code can locate both open and closed systems, and the results described here include both types. Experiments identifying only closed systems indicated little impact on the overall results. As in the divergence centers, there is no attempt to distinguish stationary and mobile systems. Once the locations were tabulated, the data were binned in 5° × 5° squares and normalized by area and time as for the 200-hPa divergence centers.

c. Normalizations

The locations of the centers of both the MSLP and the 200-hPa divergence were binned into 5° × 5° squares, and the number was normalized by the area of the square at the equator. Since the area of a 5° equatorial square is about 308,000 km² and the number of centers was summed over each season, the units of the frequency are events per season and per 308,000 km².

2. Model and Experiment Description

The model used for this experiment was the ECMWF operational model, Cycle 36. This model has 19 levels in the vertical and, for this experiment, was set to a horizontal resolution of T42. The model is in all respects the same as that described by Miller et al. (1992). This version of the model uses a gravity wave drag parameterization and a convective mass flux scheme. The T42 resolution is a compromise between the conflicting demands of sufficient resolution and realistic computation time. The work of Tibaldi et al. (1991) indicates that the T42 resolution is adequate for the type of study performed here. In the 1979 to 1988 AMIP simulation used here, the SST and sea-ice distribution used were the observed monthly values prepared for AMIP by the Center for Ocean, Land and Atmosphere at the University of Maryland and the NOAA Climate Analysis Center. The surface land temperature and moisture are allowed to vary freely in accordance to the model's surface parameterizations. The integration began with the ECMWF analysis for 1 January 1979.

3. Analysis Technique

a. 200-hPa Divergence

The upper-level wind data from the model integration were archived every 6 hr; from these data the divergence was computed and smoothed to a resolution of T30. Use of the smoothed divergence simplifies the search for maxima and minima somewhat, although small-scale divergence centers will not be detected. For the period 15 November to 15 March, the divergence fields were searched for maxima and minima, and the position of each extremum and the corresponding divergence were recorded. The criterion for an extremum was that the central point of a 5×5 array of points had to have a divergence less (or greater) than all the surrounding points. Since the grid spacing was about 2.5° in latitude and longitude, the extremum had to be at least 10° in extent to be identified. The level chosen for this work was the 200-hPa surface. This upper level is a compromise, in that a lower level would be preferable in the midlatitudes, but an upper tropospheric level is needed to capture the outflow of deep convective systems in the tropics. This upper level was also chosen in an attempt to obviate the effects of topography on the interpolation of the model's data to pressure surfaces from the model coordinates.

It should be noted that this procedure makes no distinction between stationary or slow-moving systems and fast-moving migratory storms. A stationary system will be counted more than once during its lifetime, and will thus contribute to high frequencies where such systems are endemic. The search criterion applied at 200 hPa selects only large-scale deep systems, and this must be kept in mind when interpreting the results. These restrictions on the search may be an advantage in that they focus attention on the vigorous systems that would be expected to make a substantial impact on the general circulation statistics and climatology of the model. Another possible problem is that the 200-hPa surface goes into the stratosphere at the higher latitudes. Examination of model north-south cross sections of temperature and wind (not shown) indicates that this is not a serious problem below 60° latitude.

The analysis was carried out for the 15 November through 15 March winter seasons beginning November 1980 and ending March 1988.

b. Mean Sea-Level Pressure Minima

For the same time sequence as for the 200-hPa wind field, the MSLP was calculated using the reduction procedures used at the ECMWF. MSLP minima were located and their positions recorded using the cyclone locator code developed at the University of Melbourne and described by Murray and Simmonds (1991). This code can locate both open and closed systems, and the results described here include both types. Experiments identifying only closed systems indicated little impact on the overall results. As in the divergence centers, there is no attempt to distinguish stationary and mobile systems. Once the locations were tabulated, the data were binned in $5^\circ \times 5^\circ$ squares and normalized by area and time as for the 200-hPa divergence centers.

c. Normalizations

The locations of the centers of both the MSLP and the 200-hPa divergence were binned into $5^\circ \times 5^\circ$ squares, and the number was normalized by the area of the square at the equator. Since the area of a 5° equatorial square is about 308,000 km² and the number of centers was summed over each season, the units of the frequency are events per season and per 308,000 km².

4. Results

Histograms of the divergence of all the centers identified for the eight winters analyzed were computed. The earth was divided into three regions, the Northern Hemisphere (30°N to 90°N), the Southern Hemisphere (30°S to 90S), and the tropics (30°S to 30°N). Figure 1 presents the histograms of the divergence centers and MSLP cyclones for each region. Figure 1b also shows the data of Lambert (1988), who computed cyclone locations for the Northern Hemisphere for five winters using daily ECMWF analyses. In the figure, Lambert's data have been modified to take account of the longer time period and higher sampling rate of this study. There is fair agreement between Lambert's results and those of this study, giving us some confidence in the model results in a gross sense. Figure 1 shows that the MSLP cyclones are much more numerous than the upper-level divergence centers. This is partly due to terrain and heat-flow effects in the MSLP data and partly to the fact that not all MSLP cyclones will have an identifiable signature in the 200-hPa divergence. The histograms for each individual season (not shown) for all three regions indicate that the distributions are generally stable from year to year. There was some indication that the El Niño–Southern Oscillation (ENSO) years (1982–83 and 1986–87) were periods of enhanced activity over the whole globe for both analyses.

To avoid being misled by having the results dominated by systems with negligible divergence, we plotted the frequency results of these centers using various threshold criteria. Using Fig. 1a as a guide, we created plots containing only systems whose divergence exceeded increasing values of minimum divergence (e.g., 0.2, 0.4, $0.6 \times 10^{-5} \text{ s}^{-1}$). These plots suggested that the selection of the threshold was not critical for the present purpose, and that essentially the same conclusions would be drawn using plots displaying all the centers regardless of their values.

As shown in Fig. 1b, the distributions in the different subregions are substantially different for the MSLP cyclones; this is in contrast to Fig. 1a, where the distributions for the divergence centers are quite similar. As with the divergence frequency, cyclone frequency plots were generated with various maximum-pressure cutoffs. As the histograms suggested, the cyclone frequency plots were more sensitive to the chosen threshold than the divergence plots. However, for the conclusions drawn here, a plot including all the located cyclones is adequate and is consistent with the procedure selected for plotting the divergence centers.

a. MSLP Cyclones

Figure 2a is a plot of MSLP cyclone frequency averaged over the eight winters. There appear to be high frequencies over land with high terrain (e.g., the Tibetan Plateau) and areas where heat lows are endemic (e.g., Australia). Since the analysis of MSLP in regions of elevated terrain is to a large extent arbitrary, these maxima may be artifacts. Figure 2a can be compared with published cyclone activity charts, such as that of Whittaker and Horn (1982), for monthly mean cyclone frequency over the Northern Hemisphere during 1958 to 1977. Lambert (1988) presents observational data of cyclone frequency using the ECMWF once-daily analyses of 1000-hPa geopotential for the five winters from 1980 through 1984 for the Northern Hemisphere. The Southern Hemisphere has a much smaller verification database, although the pioneering work of Taljaard (1972) for the International Geophysical Year (IGY) is still a valuable resource. Konig et al. (1991) present global frequency charts based on the ECMWF MSLP analyses for the ten winters from 1979 through 1988.

In Fig. 2a, one can readily identify the storm tracks seen in the observational data off the east coasts of the continents in the Northern Hemisphere. The Canadian Climate Model, using a resolution of T21, does not capture the Mediterranean cyclones (Lambert, 1988), whereas this model at T42 perhaps makes too much of this region. A significant difference also exists over the Middle East, where Whittaker and Horn show no activity, whereas Fig. 2a shows substantial activity. However, Lambert's analysis is more in agreement with Fig. 2a over the Middle East. Previous versions of the ECMWF model have shown a significant cyclone activity in this area that is not completely in keeping with the observations of cyclone centers (Koenig et al., 1991). Figure 2a shows a very prominent maximum near 60°N, 150°E in the Sea of Okhotsk that is much greater than the observations; this might be in part a terrain effect. On the whole, however, Fig. 2a indicates that the model does a credible job with respect to the location and frequency of MSLP cyclones in the Northern Hemisphere.

In the Southern Hemisphere, the cyclone frequencies of Fig. 2a are similar to those found in the ECMWF analysis for the winters from 1979 through 1988 by Konig et al. (1991), although the maxima projecting eastward from New Zealand, Argentina, and South Africa are more prominent in Fig. 2a. The tongue of cyclone activity extending along 15°S to the west of Madagascar appears to be excessive, since it is not significant in the observational data of Konig et al. (1991). The Indian Ocean in this region is the only place in the tropical band with significant MSLP cyclone activity in the model simulation. Although Taljaard's (1992) data indicate a maximum extending southeast over the Atlantic from South America, Taljaard reports that this

feature is more prominent in the southern winter. Koenig et al. (1991) also note that their earlier version of the ECMWF model has an erroneously large area of cyclonic activity extending southeastward from Brazil. From the rather meager data available, it can be concluded that the model does an adequate job in describing the cyclone activity in the Southern Hemisphere.

b. 200-hPa Divergence Centers

A primary reason for presenting the MSLP cyclone frequencies is to compare them with the 200-hPa divergence-center frequencies shown in Fig. 2b. Both Figs. 2a and 2b show a midlatitude maximum over the North Pacific basin, but the divergence-center maximum is shifted equatorward with respect to the cyclone frequency in the western Pacific. The divergence centers tend to be closer to the cyclonic shear side of the east Asian jet maximum, whereas in the Atlantic the cyclone and divergence maxima more nearly coincide. There is a noticeable discrepancy between Figs. 2a and 2b off the southern tip of Greenland, but the cyclones generated there are probably forced by the orography and are not deep enough to show up at 200 hPa. It therefore appears that the 200-hPa divergence centers display a useful correspondence to the MSLP cyclones.

Another possible data set for comparison with Fig. 2b in midlatitudes is the variance of the upper-level heights. The regions of high upper-level variability, as indicated by the standard deviation of the twice-daily 300-hPa geopotential, have been identified with storm tracks as the transient systems move and develop in the westerlies. Figure 2b is in general agreement with the regions of enhanced upper-level geopotential variability shown by Lau et al. (1981) in their comprehensive atlas of the geopotential variations at the 300-hPa level. It should also be noted that the 1000- and 300-hPa geopotential variance data of Lau et al. display a relative spatial relation similar to that seen in Figs. 2a and 2b over the North Pacific.

In the tropics, the MSLP cyclone signal is slight, but the divergence centers are prominent. The major convective centers over Indonesia, the Indian Ocean, South America, and Africa are evident in Fig. 2b. The tropical patterns can be compared with patterns of observed outgoing longwave radiation (OLR), assuming that the divergence centers will be regions of high clouds and thus of reduced OLR. According to the data of Janowiak et al. (1985), this is in fact the case. The frequency of divergence centers in the tropics can also be compared with the frequency of highly reflective cloud (HRC), which indicates regions of deep convection. Garcia (1985) presents HRC mean monthly fields and coefficients of variability for the tropical band 30°N to 30°S during 1971–83 based on daily satellite observations. Figure 2b generally agrees well with the

HRC data presented by Garcia (1985), although the prominent maximum extending eastward from New Guinea to the dateline in the HRC data is somewhat muted in Fig. 2b. The maximum in southern Africa in Fig. 2a appears to be displaced to the southeast with respect to the HRC maximum, and the center near Central America seems to be too far to the northeast of the observed HRC maximum, which is just off the Equadorian coast; the model appears to underestimate the centers over Amazonia near 10°S in the HRC. The HRC data, however, have a definite signal at 150°W along the equator, in agreement with Fig. 2b.

For an additional comparison in the Southern Hemisphere, Trenberth (1991) provides charts of the band-pass filtered (2 to 8 days) height variance at 300 hPa for January 1979–89, using the ECMWF operational analysis. The band-pass filter restricts the data to transient disturbances and removes the stationary features. Trenberth's data and Figs. 2a and 2b exhibit a similarity in that there are minima of activity from the Chilean coast west to about 150°W and there is a modest maximum in both fields in the southern Indian Ocean. The model has very little activity in the South Atlantic from 0 to 40°E, while Trenberth's data indicate a band from 40°E to 60°W.

Figure 3 is obtained by plotting only centers with divergence greater than $0.4 \times 10^{-5} \text{ s}^{-1}$. Only a few strong events are found in the tropics over the Pacific or Atlantic Oceans; the largest values are over Africa, South America, the maritime continent, and the Indian Ocean just south of the Bay of Bengal. With the exception of the Indian Ocean, the tropical strong events are restricted to land areas, whereas the strong divergence centers are chiefly over the oceans in the midlatitudes but are more land-based in the tropics. The distribution of midlatitude events in Fig. 3 can be compared with the wintertime Northern Hemisphere climatology developed by Roebber (1984) for explosively developing cyclones. It would seem reasonable that most rapidly developing cyclones would be accompanied by significant upper-level divergence. The overall contours of Fig. 3 agree with Roebber's analysis in that the regions of frequent strong upper-level divergence coincide with the regions where explosively developing cyclones are found. However, Roebber identifies the highest frequency as occurring east of Japan at 150°E, 40°W, which is not a maximum in Fig. 3.

c. *Interannual Variability*

Since this model simulation used the observed monthly averaged observed SSTs, it is of interest to investigate the interannual variability of the model. Figure 4 presents the standard deviation of the divergence centers and the MSLP cyclones for the eight seasons of data. With regard to the midlatitudes, the Northern Hemisphere

storm tracks are regions of enhanced variability, whereas the southern (summer) tracks have less interannual variability. There is also considerable variability in the tropical Indian Ocean and along the SPCZ. The dominant centers in Fig. 4b are the tropics. Two of those centers, the region over Indonesia and that near the dateline, are presumably linked to ENSO events. On the whole, the regions of tropical variability correlate well with observations of OLR variability (Janowiak et al., 1985). One might speculate that the large tropical variability extending from Africa across the Indian Ocean to the dateline might also be related to the intraseasonal (30–40 day) oscillation, whose activity varies greatly from year to year (Philander, 1990).

d. Anomalies

Another aspect of the interannual variability is the anomalies of the individual seasons with respect to the eight-season mean. Figure 5 presents the plots of the distribution of the anomaly divergence-center frequency and MSLP cyclone frequency for the winters of two ENSO maxima of 1982–83 and 1986–87 and the ENSO minima of 1984–85. These anomalies can be viewed as part of the dynamical global response of the model to the varying SST. For this single realization, however, it is not possible to completely untangle the intrinsic variability of the model from that forced by the SST changes.

Looking at Figs. 5a, 5b, 5e, and 5f, which are the divergence and cyclone frequency anomalies corresponding to the El Niño periods, one can discern similarities in the two seasons. In the divergence-center plots (Fig. 5e and 5f), there is evidence of an enhancement in the equatorial convective centers in the central Pacific, which could be considered directly driven by the SST anomalies. This pattern is quite apparent in the OLR and HRC data for these winters. In the 1986–87 winter, two maxima exist near the equator at 135°W, whereas in 1982–83 a single center exists; the South Pacific Convergence Zone (SPCZ) is more prominent in 1986–87. In both seasons, the tropical Atlantic has a frequency maximum just poleward of the equator. There is also some evidence that the model is depicting the midlatitude ENSO effects correctly. There is a small enhancement of activity over the coast of California and a substantial increase east of Florida. Using precipitation anomaly data, Ropelewski and Halpert (1989) identified the U.S. southeastern coast as a key region of wintertime response to ENSO events. They found a significant increase in wintertime precipitation in this region during ENSO events. Figure 5d also indicates that the Atlantic storm track has shifted equatorward in this winter (1982–83). The prominent decrease in activity over South America from the equator to 15°S in 1982–83 is also in accord with observations. These

charts can be contrasted with Fig. 4e, which corresponds to the winter of 1984–85, a period of cold anomalies in SST along the equator. Activity is suppressed almost globally in the northern storm tracks except over the Indian Ocean and Brazil.

The anomalous cyclone frequency charts show some interesting relations to the divergence-center data. In Fig. 4b, the prominent maxima in the divergence-center anomalies near the dateline and near 135°W and 30°W along the equator are not reflected in the SLP cyclone frequencies. Yet in the tropical Indian Ocean, there appears to be a correspondence between the SLP and divergence extrema, which in the middle latitudes appears to be more consistent. There is also an increase in the cyclone activity off the west coast of the U.S. and over the southeast U.S., concomitant with the divergence centers in 1982–83 and 1986–87. There are also regions in which the two fields have opposite signs, such as in the eastern North Atlantic.

e. Convergence Centers

The convergence centers have received somewhat less attention. Nonetheless, where descent and dry conditions prevail is of as much interest as divergence centers to where rain falls in the proper specification of the global climate.

f. Frequency

Figure 6 shows the normalized divergence-center frequency and standard deviation for convergence centers. In Fig. 6a, the subtropical high-pressure belts are clearly in evidence around 30°N and 30°S. In the tropics, the active divergence regions are seen as regions of little convergent activity, whereas in the midlatitudes (especially off the east coast of the continents), there tends to be more mixing, as can be seen by comparing Figs. 6a and 2b. There is also a maximum of convergence associated with moderately strong divergence centers in the lee of the Rockies and the Tibetan Plateau. In these regions, the convergence associated with outbreaks of cold air is also a region of lee cyclone development and upper-level divergence. In the midlatitude storm tracks, the convergence centers tend to be equatorward of the divergence centers—this is the same relation observed in cyclone–anticyclone couplets. The standard deviation given in Fig. 6b shows that the convergence centers have slightly less variability. There is also some indication that the variations of the divergence-center frequency from 15°E to 150°E in the tropics are matched by variations in the convergence-center frequency on either side of this maximum.

5. Discussion

The major point made in this work is the usefulness of the upper-level divergence-center frequency in depicting the global aspects of model dynamics that are useful for model intercomparison. In comparing a large number of models in a project such as AMIP, the ability to make meaningful conclusions using a single scalar field of global extent is a useful diagnostic.

Hoerling et al. (1992) present the results of a simulation of the 1985–86 and 1986–87 northern winters using the NCAR Community Climate Model (CCM1). In the simulation, the observed SST was used as in the experiment described in this paper. Hoerling et al. state that the simulation of the 1986–87 winter is somewhat more like the available observations than is that of the 1985–86 winter. They present plots of the simulated and observed (NMC analyses) seasonally averaged divergence for both winters. If it is assumed that the plots of divergence-center frequency correspond to the mean divergence plots, similar conclusions can be drawn from the present simulation, in which the 1986–87 winter corresponds fairly well with the observations and the 1985–86 winter does not. It is perhaps significant that both models, CCM1 and ECMWF, show more activity across the Indian Ocean from Southern Africa to Indonesia than the observations in both years. Since this band of activity is presumably dominated by convective activity, it should be noted that the two models have significantly different cumulus parameterizations. [The CCM1 uses a convective adjustment scheme, whereas the ECMWF model incorporates the Tiedtke (1989) mass flux scheme.]

Figure 7 shows the mean 200-hPa divergence for the eight winters for the model simulation. If one combines Fig. 2b (the divergence-center frequency) and Fig. 6a (the convergence-center frequency), the result would look much like Fig. 7. This relation also holds for anomaly plots of the divergence for individual winters (not shown). There does not appear to be an overwhelming *a priori* reason why this should be so. At least in midlatitudes, it would seem that a region of a high number of divergence centers need not be a region of large mean divergence if the region alternates between convergence and divergence as the transient centers pass through it. Evidently the dominant systems in the divergence- and convergence-center statistics are quasi-stationary. This can be seen in Fig. 2b, in that there are dipoles of maxima and minima about the entrance and exit regions of the major jet axes over east Asia and eastern North America. The quasi-steady nature of the major convective centers over tropical Africa, Indonesia, and South America is also obvious in the figures.

What, then, is to be gained by calculating the individual centers rather than calculating only the monthly mean divergence? Figure 3 illustrates one advantage, in that we can stratify the systems by their magnitude to gain some insight as to how the mean fields are obtained by the model. Tracking the centers would allow analysis of the paths of the centers and separation of the mobile systems from the stationary ones. These types of analysis will become even more valuable as re-analyses permit a similar analysis to be performed on the observations.

In summary, the centers of divergence and convergence at 200 hPa and the MSLP cyclones identified for the northern winter in a GCM simulation extending from 1980 to 1988 yield the following conclusions:

1. The model achieves a reasonable simulated climatology of MSLP cyclones and upper-level divergence.
2. There is a good correspondence between the seasonally averaged upper-level divergence-center frequency and MSLP cyclone frequency.
3. The model appears to respond realistically, on a global scale, to the variations in SST, at least to the extent that the observations permit.
4. The tropical Indian Ocean is the region of greatest variability in the frequency of divergence centers.
5. Response to the two ENSO events modeled (1982–83 and 1986–87) is not uniform over the globe.
6. Analysis of upper-level divergence centers would prove useful in comparing GCM integrations and their response to varying SST.
7. The convergence centers display a smaller interannual variability compared to that of the divergence centers.

Acknowledgments: The cooperation of the ECMWF in making their forecast model available and in providing expert technical advice for this research is gratefully acknowledged. I am indebted to Ian Simmonds and David Jones of the University of Melbourne for supplying me with their cyclone locator code; Dr. Jones supplied invaluable help in getting the code running. This work was performed under the auspices of the U.S. Department of Energy Environmental Sciences Division by the Lawrence Livermore National Laboratory under contract W-7405-ENG-48.

REFERENCES

- Garcia, O., 1985: Atlas of highly reflective clouds for the global tropics: 1971–1983. NOAA Environmental Research Laboratories, Boulder, CO, 365 pp.
- Gates, W. L., 1992: AMIP: The Atmospheric Model Intercomparison Project. *Bull. Am. Met. Soc.* **73**, 1962–1970.
- Hoerling, M. P., M. L. Blackmon, and M. Ting, 1992: Simulating the atmospheric response to the 1985–87 El Niño cycle. *J. Climate* **5**, 669–682.
- Hsu, H.-H., and S.-H. Lin, 1992: Global teleconnections in the 250-mb streamfunction field during the northern hemisphere winter., *Mon. Wea. Rev.* **120**, 1169–1190
- Janowiak, J. E., A. F. Krueger, and P. A. Arkin, 1985: Atlas of outgoing longwave radiation derived from NOAA satellite data. NOAA Atlas No. 6, U. S. Dept. of Commerce, Silver Spring, MD, 44 pp.
- Kalnay, E., and R. Jenne, 1991: Summary of the NMC/NCAR reanalysis workshop of April 1991. *Bull. Am. Meteor. Soc.* **72**, 1897–1904.
- Koenig, W., R. Sausen, and F. Sielmann, 1991: Objective identification of individual cyclones in a climate model. In *Meteorologisches Institut der Universitat Hamburg*, Rept. No. 9, Hamburg, FRG, 99–113. [Available from Meteorologisches Institut der Universitat Hamburg, Bundesstr 55, D-2000, Hamburg 13, F. R. Germany]
- Lambert, S. J., 1988: A cyclone climatology of the Canadian Climate Centre general circulation model. *J. Climate* **1**, 109–115.
- Lau, N.-G., G. H. White, and R. L. Jenne, 1981: Circulation Statistics for the extratropical northern hemisphere based on NMC analyses. NCAR/TN-171+STR, National Center for Atmospheric Research, Boulder, CO, 138 pp. [Available from National Center for Atmospheric Research, Information Services, P.O. Box 3000, Boulder, CO 80307.
- Miller, M. J., A. C. M. Beljaars, and T. N. Palmer, 1992: The sensitivity of the ECMWF model to the parameterization of evaporation from the tropical oceans. *J. Climate* **5**, 418–434.
- Murray, R. J., and I. Simmonds, 1991: A numerical scheme for tracking cyclone centres from digital data. Part I: Development and operation of the scheme. *Aust. Met. Mag.* **39**, 155–166.
- Petterssen, S., 1956: *Weather Analysis and Forecasting*, Vol. 1, McGraw-Hill, 422pp.
- Philander, S. G., 1990: *El Niño, La Niña, and the Southern Oscillation*. International Geophysics Series **46**, Academic Press, New York, 293 pp.

- Roebber, P. J., 1984: Statistical analysis and updated climatology of explosive cyclones. *Mon. Wea. Rev.* **112**, 1577–1586.
- Ropelewski, C. F., and M. S. Halpert, 1989: Precipitation patterns associated with the high index phase of the Southern Oscillation. *J. Climate*, **2**, 268–284.
- Taljaard, J. J., 1972: Synoptic meteorology of the Southern Hemisphere, in *Meteorology of the Southern Hemisphere* (ed. C. Newton), Meteorological Monographs **13(35)**, American Meteorological Society, Boston, MA, 263 pp.
- Tibaldi, S., T. N. Palmer, C. Brankovic and U. Cubasch, 1990: Extended-range predictions with ECMWF models: Influence of horizontal resolution on systematic error and forecast skill, *J. Roy. Met. Soc.* **116**, 835–866.
- Tiedtke, M., 1989: A comprehensive mass flux scheme for cumulus parameterization in large-scale models. *Mon. Wea. Rev.*, **117**, 1777–1798.
- Trenberth, K., 1991: Storm tracks in the Southern Hemisphere. *J. Atm. Sci.* **48**, 2159–2178.
- Whittaker, L. M., and L. H. Horn, 1982: *Atlas of Northern Hemisphere Extratropical Cyclone Activity, 1958–1977.*, Dept. Of Meteorology, University of Wisconsin, Madison, WI, 65 pp.

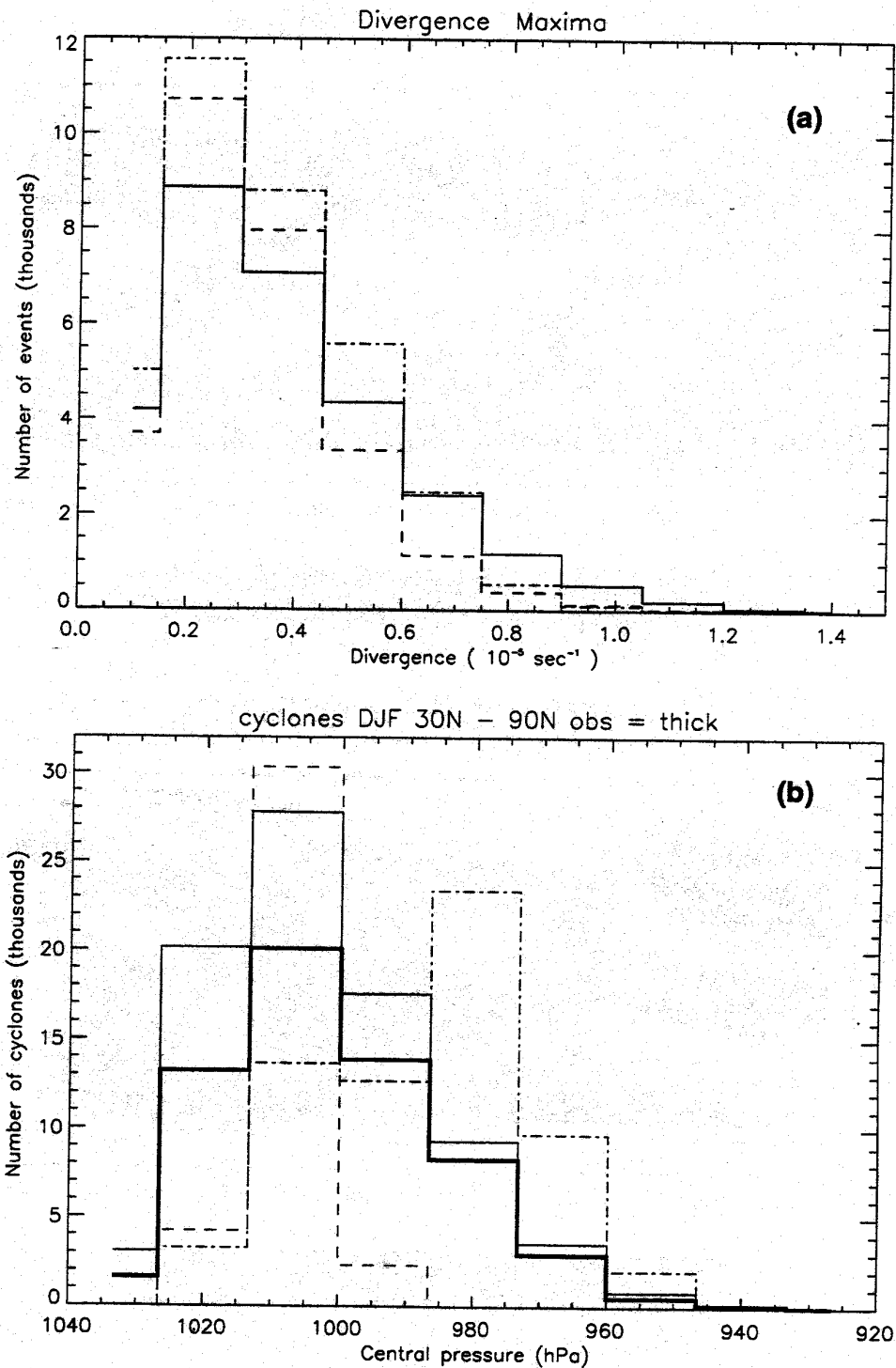
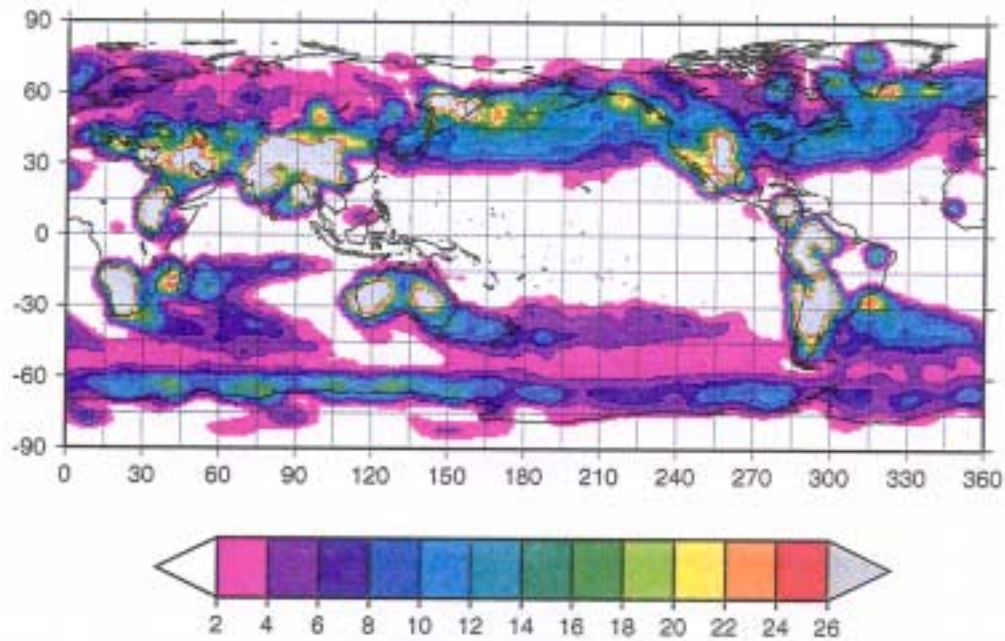


Fig. 1. (a) Magnitude of the divergence centers identified for the northern winter in the northern hemisphere (30°N to 90°N; solid line), the southern hemisphere (30°S to 90°S; dash-dot line), and the tropical region (30°S to 30°N; dashed line). (b) As in (a) except for the MSLP cyclones. The thick solid line is the data from Lambert (1988), using ECMWF analyses.

(a)

Cyclone frequency



(b)

Divergence frequency

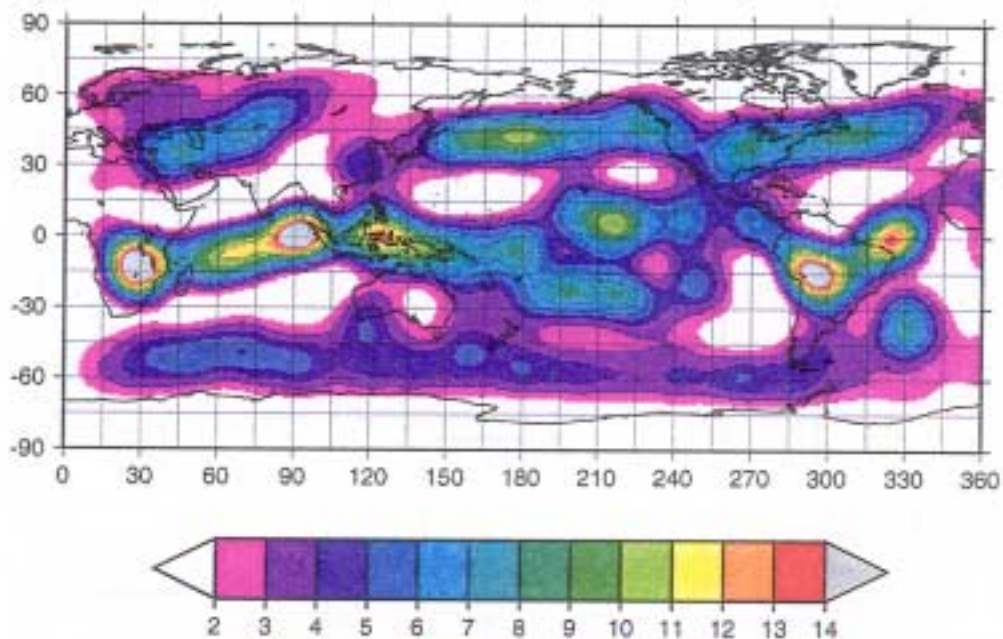


Fig. 2. (a) Number of MSLP cyclones per winter and per 308,000 km², averaged over the eight northern winters from 1980–88. The contour interval is 2. Regions of mean surface elevation greater than 1500 m are blanked out. (b) As in (a) except for 200-hPa divergence centers.

Divergence frequency

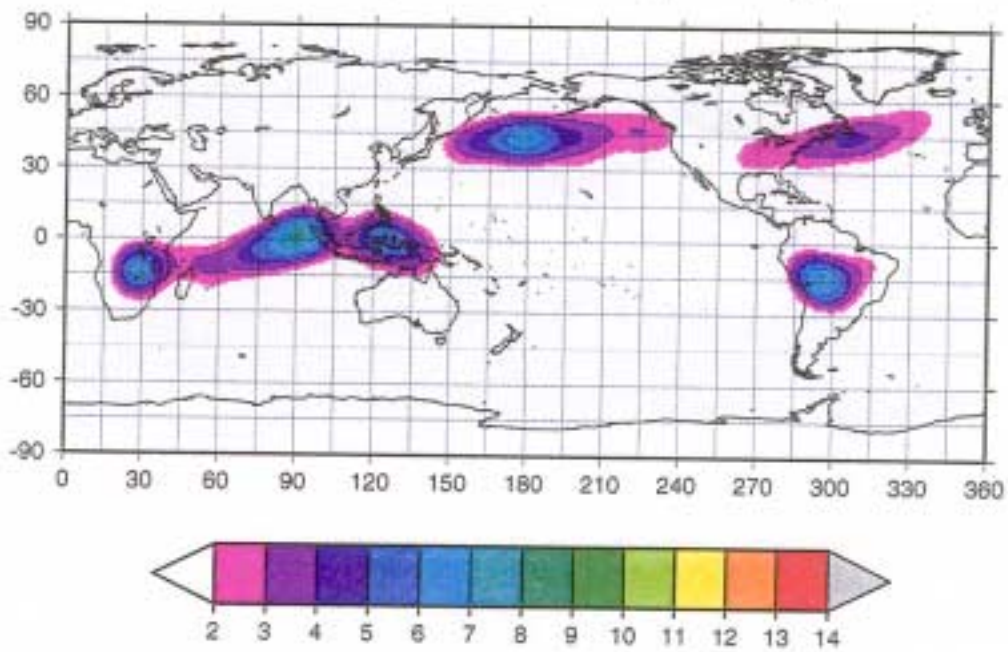
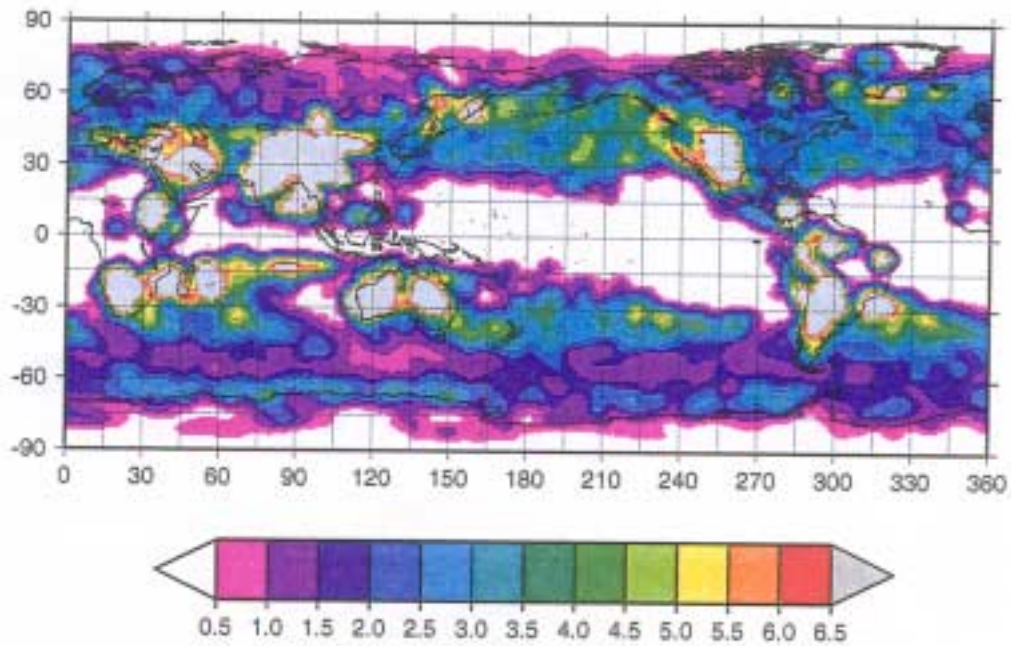


Fig. 3. Number of strong ($>0.4 \times 10^{-5} \text{ s}^{-1}$) 200-hPa divergence centers per winter and per 308,000 km², averaged over the eight northern winters from 1980–88. The contour interval is 1.

(a) Standard deviation - cyclones



(b) Standard deviation - divergence

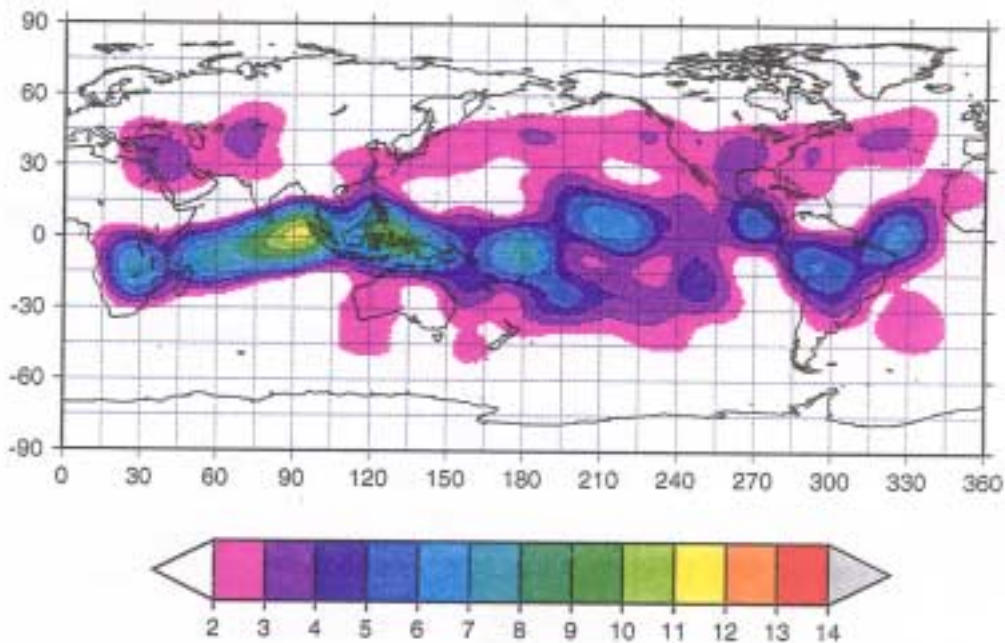
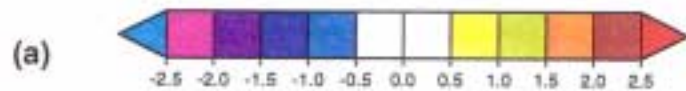
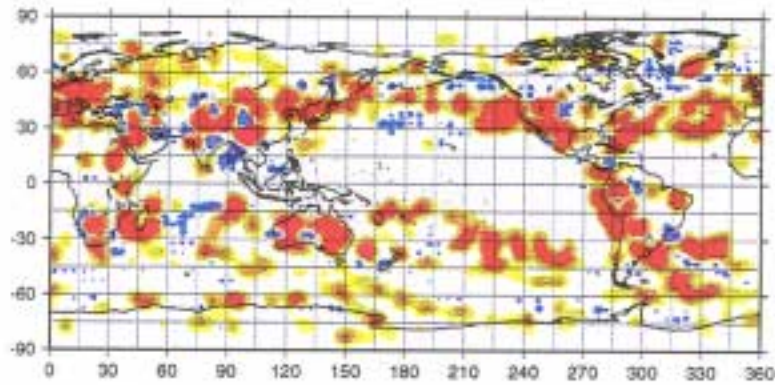
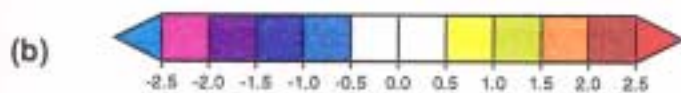
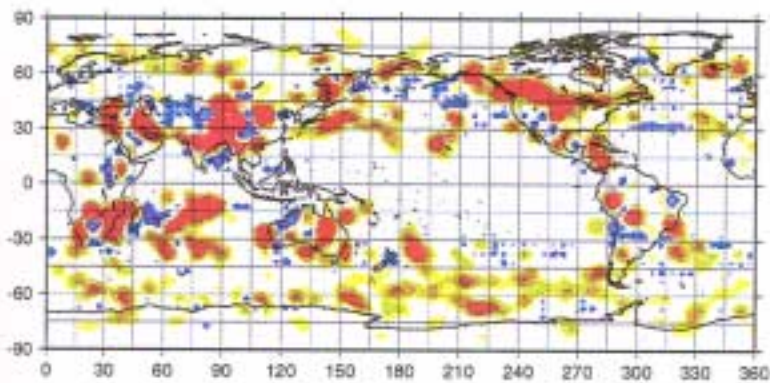


Fig. 4. Standard deviation of the number of MSLP cyclones per winter and per 308,000 km², averaged over the eight northern winters from 1980-88. The contour interval is 0.7. (b) As in (a) except for 200-hPa divergence centers.

Cyclone frequency anomaly 8283



Cyclone frequency anomaly 8485



Cyclone frequency anomaly 8586

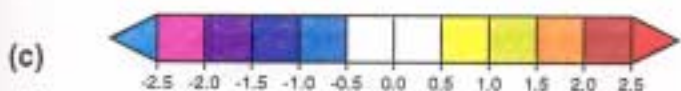
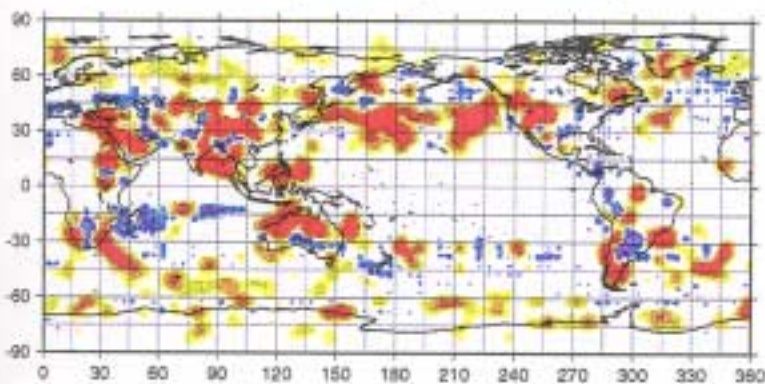
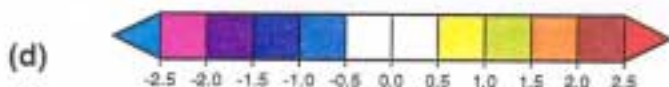
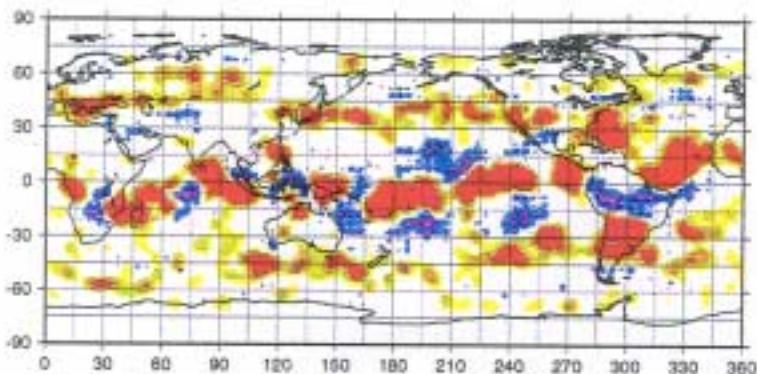
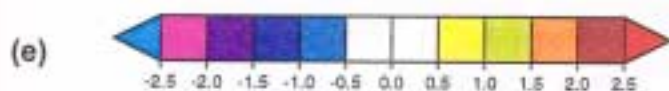
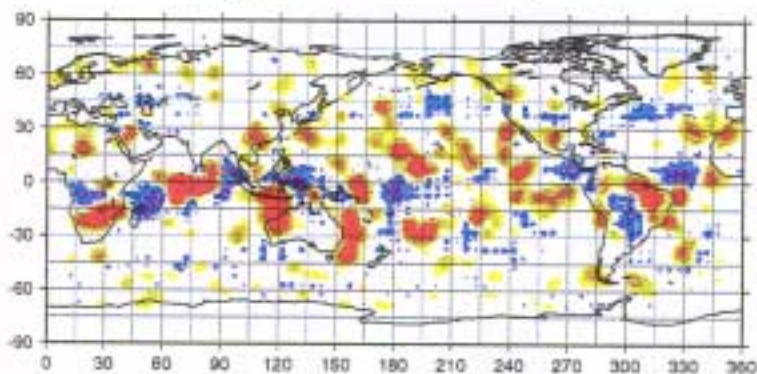


Fig. 5(a) Anomaly for the 1982-83 winter MSLP cyclone frequency, computed as the difference from the mean of the eight northern winters from 1980-88. Contour interval is 2. (b) As in (a) except for 1984-85. (c) As in (a) except for 1985-86.

Divergence anomaly 8283



Divergence anomaly 8485



Divergence anomaly 8586

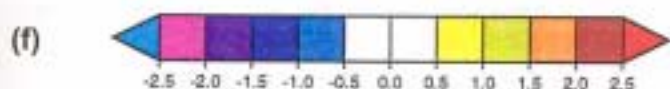
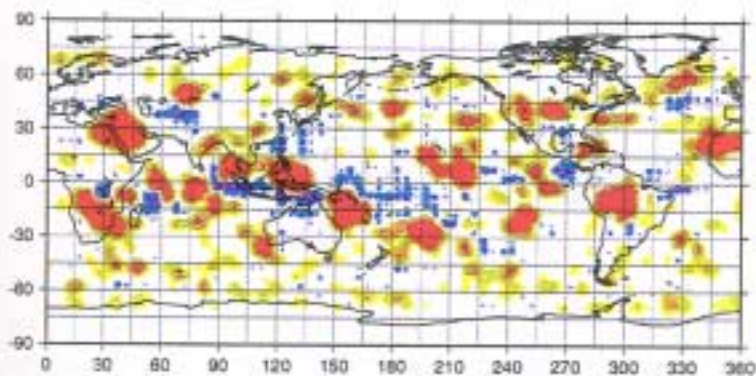
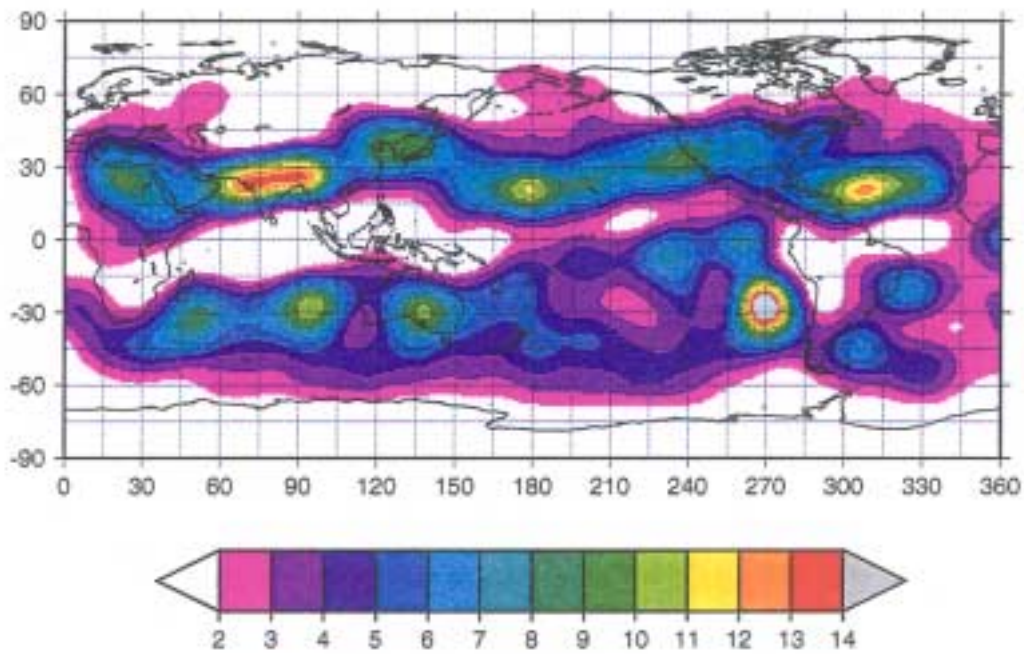


Fig. 5(d) Anomaly for the 1982-83 winter 200-hPa divergence center frequency, computed as the difference from the mean of the eight northern winters 1980-88. Contour interval is 2. (e) As in (d) except for 1984-85. (f) As in (d) except for 1985-86.

(a) Convergence frequency



(b) Standard deviation convergence

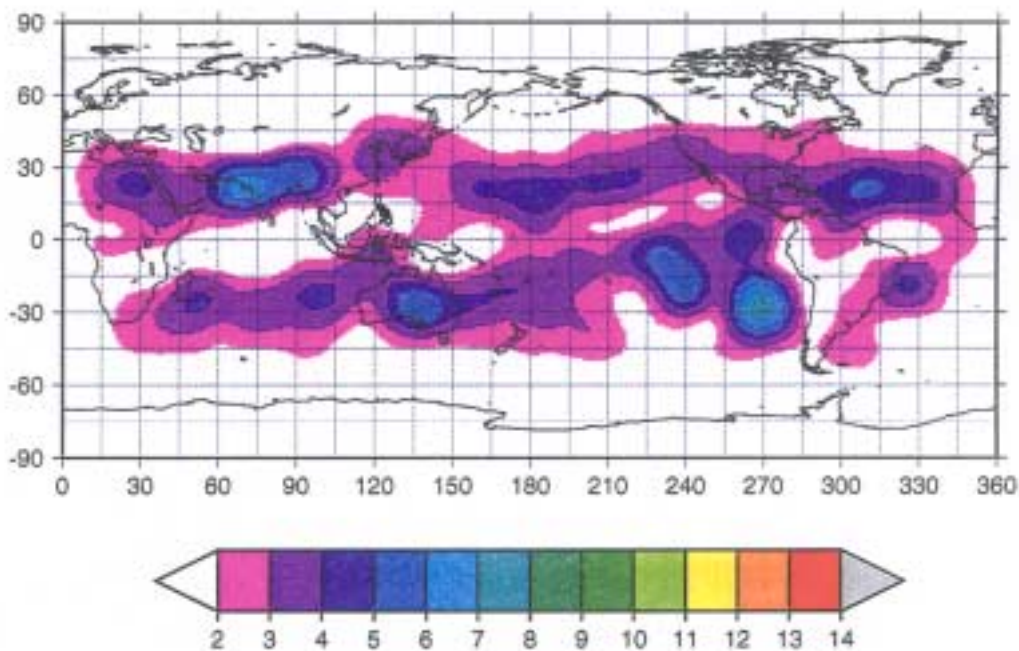
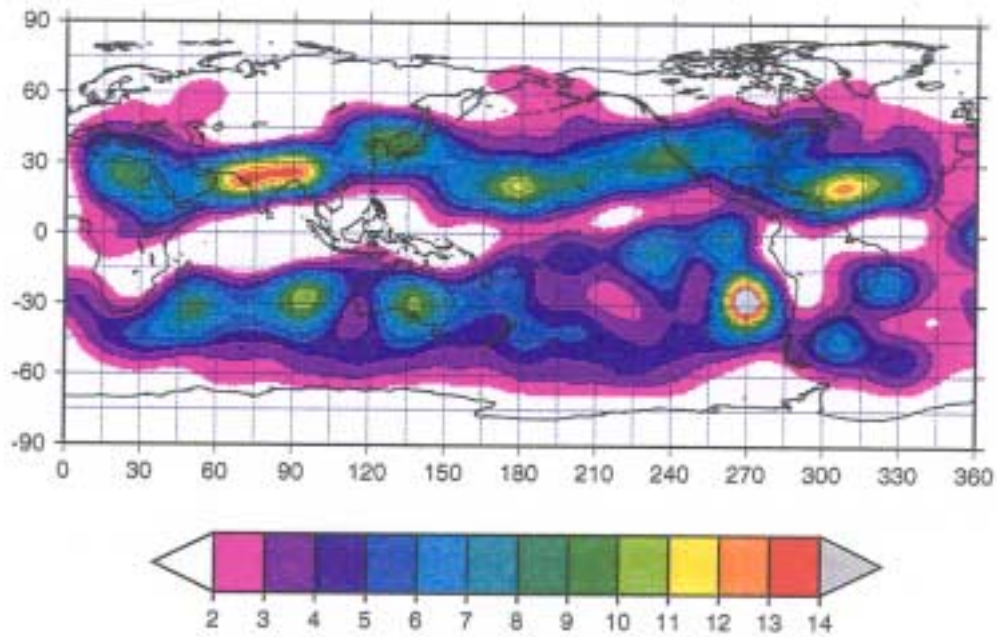


Fig. 6. (a) Number of 200-hPa convergence centers per winter and per 308,000 km², averaged over the eight northern winters from 1980–88. The contour interval is 2. (b) Standard deviation of the number of 200-hPa convergence centers per winter and per 308,000 km², averaged over the eight northern winters from 1980–88. The contour interval is 0.7.

(a) Convergence frequency



(b) Standard deviation convergence

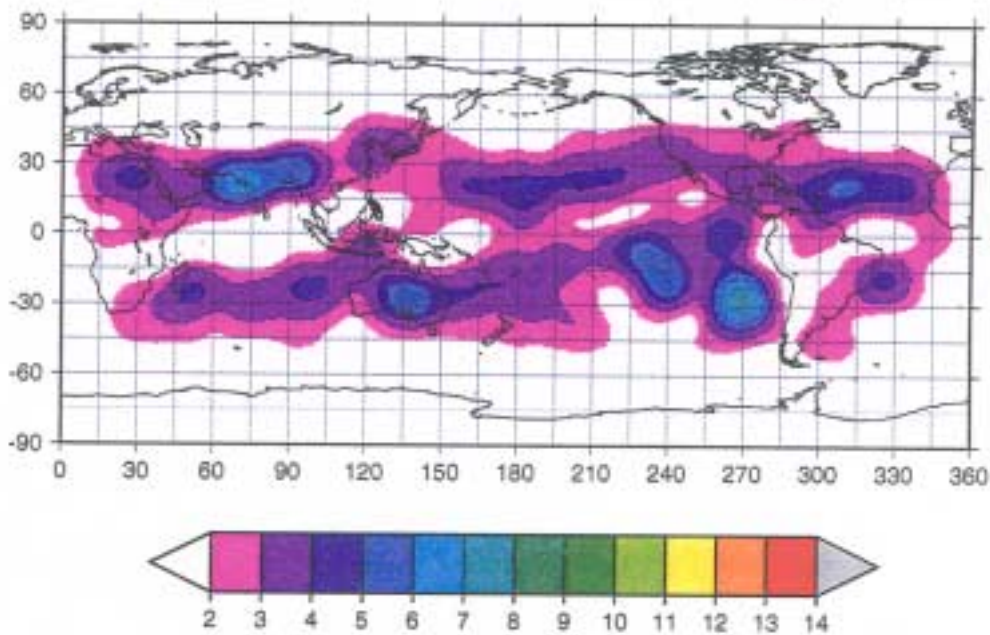
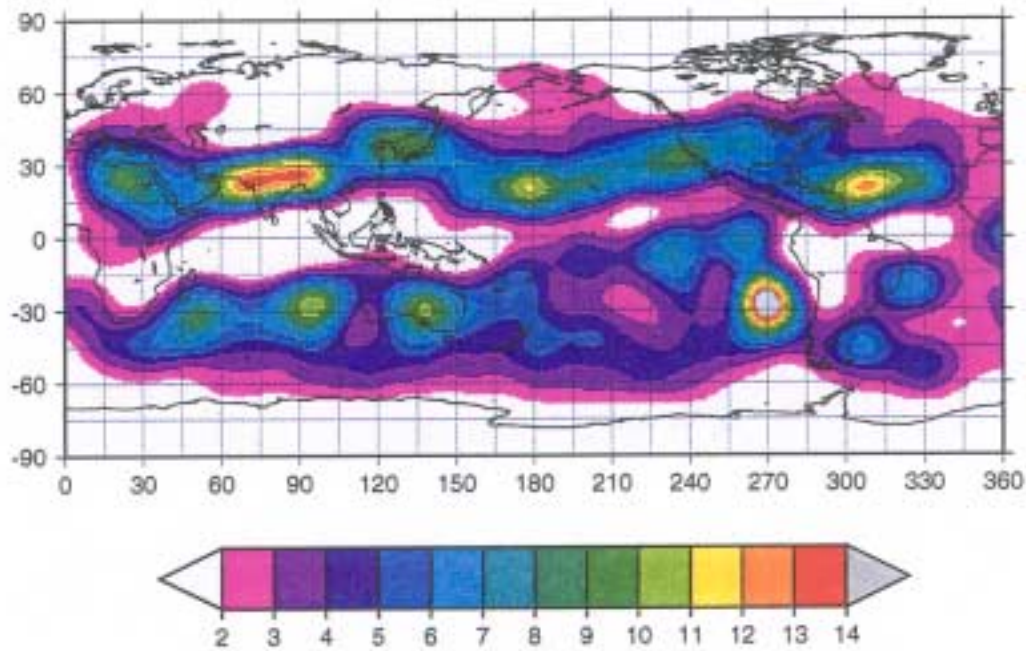


Fig. 6. (a) Number of 200-hPa convergence centers per winter and per 308,000 km², averaged over the eight northern winters from 1980–88. The contour interval is 2. (b) Standard deviation of the number of 200-hPa convergence centers per winter and per 308,000 km², averaged over the eight northern winters from 1980–88. The contour interval is 0.7.

(a) Convergence frequency



(b) Standard deviation convergence

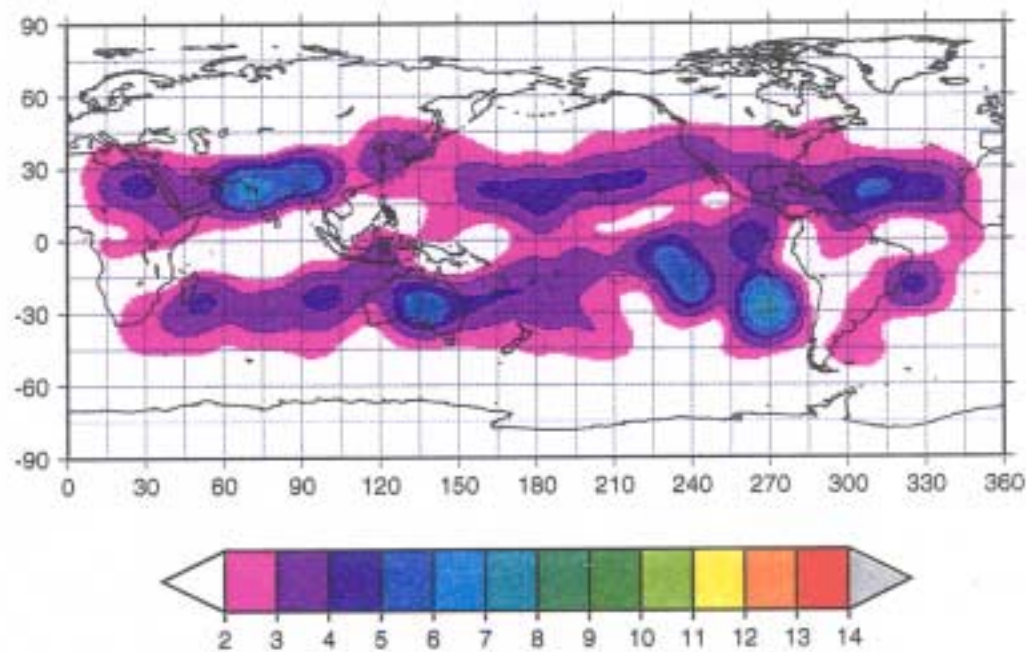


Fig. 6. (a) Number of 200-hPa convergence centers per winter and per 308,000 km², averaged over the eight northern winters from 1980–88. The contour interval is 2. (b) Standard deviation of the number of 200-hPa convergence centers per winter and per 308,000 km², averaged over the eight northern winters from 1980–88. The contour interval is 0.7.

Mean divergence

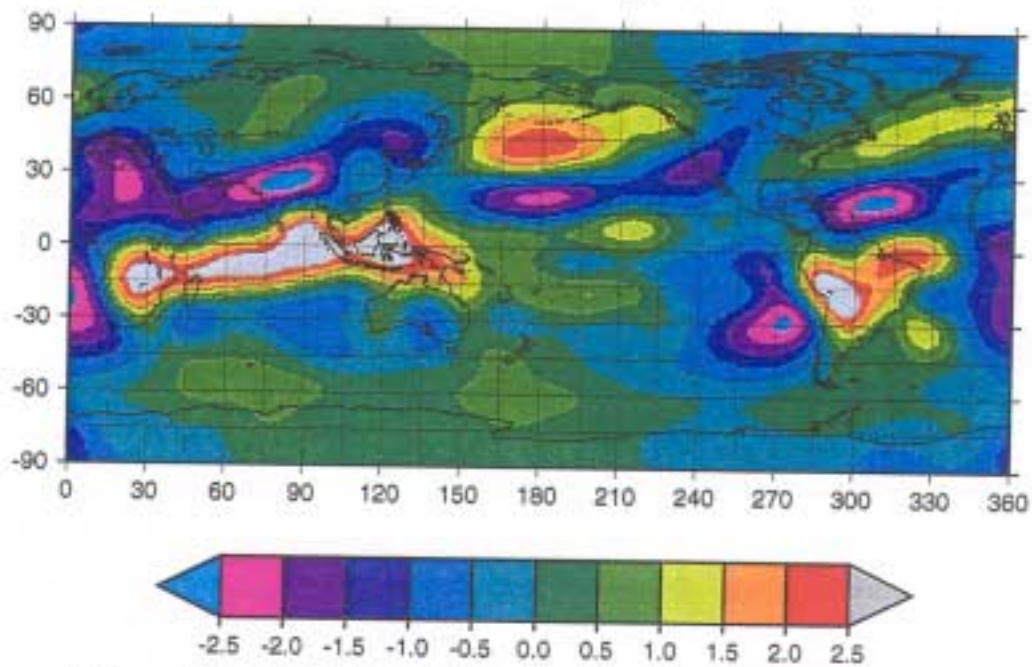


Fig. 7. The model-simulated 200-hPa mean divergence, averaged over the eight northern winters from 1980–88. The contour interval is $0.5 \times 10^{-5} \text{ s}^{-1}$. Solid contours indicate positive values (divergence) and dashed contours indicate negative values (convergence).